

University at Albany, State University of New York

Scholars Archive

Anthropology

Honors College

Fall 12-2018

RACK1 Facilitates Efficient Translation of Viral and Cellular IRESs

Natasha Permaul

University at Albany, State University of New York, npermaul@albany.edu

Follow this and additional works at: https://scholarsarchive.library.albany.edu/honorscollege_anthro



Part of the [Biological and Physical Anthropology Commons](#)

Recommended Citation

Permaul, Natasha, "RACK1 Facilitates Efficient Translation of Viral and Cellular IRESs" (2018).
Anthropology. 26.

https://scholarsarchive.library.albany.edu/honorscollege_anthro/26

This Honors Thesis is brought to you for free and open access by the Honors College at Scholars Archive. It has been accepted for inclusion in Anthropology by an authorized administrator of Scholars Archive. For more information, please contact scholarsarchive@albany.edu.

RACK1 Facilitates Efficient Translation of Viral and Cellular IRESs

An honors thesis presented to the
Department of Human Biology,
University at Albany, State University of New York
in partial fulfillment of the requirements
for graduation with Honors in Human Biology
and
graduation from the Honors College

Natasha Permaul

Research Mentor: Dr. Gabriele Fuchs, Ph.D.
Second Reader: Lawrence, Schell, Ph.D.

December 2018

Abstract

Ribosomes, the cellular machinery that translates mRNA sequences into protein sequences, are surprisingly heterogeneous molecules. More and more ribosomal proteins have been shown to facilitate translation of mRNA subsets. These mRNA subsets include mRNAs that can initiate translation using non-canonical pathways, for example using an internal ribosome entry site (IRES). IRESs are RNA structures that facilitate translation with fewer translation initiation factors than are required for canonical cap-dependent translation initiation. The ribosomal protein Receptor for Activated C Kinase 1 (RACK1) has been previously shown to be required for translation of the hepatitis C virus (HCV) IRES, but not required for translation of the intergenic IRES of cricket paralysis virus (CrPV).

We tested if RACK1 is generally required for translation of IRES-containing mRNAs by employing dual-luciferase constructs. These constructs allow us to measure cap-dependent and IRES-dependent translation from the same sample, even from the same mRNA. Using haploid 1 wildtype, RACK1 knockout cells generated by CRISPR-Cas9 mediated genome editing, and RACK1 add-back cell lines, we investigated if RACK1 is also required for translation of other viral IRESs, specifically encephalomyocarditis Virus (EMCV) and poliovirus (PV). Indeed, PV and EMCV also require RACK1 for efficient IRES translation.

Further, certain cellular mRNAs also contain IRESs, which allow these mRNAs to be translated under conditions of stress. We next tested if the cellular IRESs myb, L-myc, Bag-1, cyclin D, c-myc, and Set7 also require RACK1 for translation. Interestingly, we found that translation of all cellular IRESs we tested was also decreased in cells lacking RACK1. Overall, in cells lacking RACK1 translation of all tested viral and cellular IRESs is decreased and translation efficiency can be mostly partially or fully rescued in RACK1 knockout cells that express RACK1.

Acknowledgements

Research has opened so many doors for me, ones that I could not open on my own and has impacted the direction I would like to head in my future career. I would like to acknowledge and thank the following important people who have continuously supported me not only during my work on this thesis but throughout all my undergraduate endeavors.

Firstly, I express my sincere gratitude to Dr. Gabriele Fuchs who accepted me into her lab to work under her guidance on an array of projects. Her mentorship has extended beyond the lab and for that I am so grateful. And how can I forget her delectable cakes that always added a sweet taste to lab meetings?

I would like to thank a graduate student Ethan LaFontaine for assisting me in this research project. I am appreciative to Clare Miller who shared her knowledge in the field of research and for all her insights during my course of stay here. She started off as the cool introduction to biology lab TA and has ended off as an extraordinary caring friend. I especially thank Dr. Sangeetha Selvam for providing me with all the IRES structures and for always having an infectious smile on her face. I would also like to thank my lab members who provided me with an encouraging environment and made me feel that I was never alone for the past two years. Before being a part of this lab, I did not feel like I held a specific place at this University but since then, it has become my home-away-from-home.

Lastly, I would like to thank my friends and family. Tamara McLean, Zibby Eckhardt, and Eden Alin have all been strong roots that have kept me grounded in the stormy weather. A special thanks to my parents who transcended me to the place that I currently am. Without their endless counsel, I would not have pushed myself to always do my best. Of course, all that I have accomplished in my 21 years of life has been because of my God.

Table of Contents

| | |
|----------------------------|-----|
| Abstract | ii |
| Acknowledgments | iii |
| Table of Contents | iv |
| List of Figures | v |
| List of Tables | vi |
| List of Appendices | vii |
| Introduction | 1 |
| Material and Methods | 13 |
| Results | 18 |
| Discussion | 27 |
| Conclusion | 29 |
| Future Implications | 30 |
| References | 31 |
| Appendices | 36 |

List of Figures

| | |
|--------------------------------------------------------------------------------------------|----|
| Figure 1: Cartoon Structure of Mature mRNA | 1 |
| Figure 2: Required Initiation Factors for Cap-dependent Translation..... | 2 |
| Figure 3: Cartoon Structure of Mature mRNA with IRES in 5' UTR | 2 |
| Figure 4: Required Initiation Factors for HCV IRES-dependent Translation | 3 |
| Figure 5: Class IV CrPV _{IGR} IRES Requiring No Initiation Factors | 5 |
| Figure 6: Class III HCV IRES Showing No Initiation Factors | 5 |
| Figure 7: Class I PV IRES Showing No Initiation Factors | 6 |
| Figure 8: Class II EMCV IRES Showing No Initiation Factors | 7 |
| Figure 9: Structure of Cellular IRES cmc8 | 8 |
| Figure 10: Cartoon Depiction of IRES _{HCV} -Bicistronic Luciferase Reporter | 13 |
| Figure 11: Cartoon Illustration of SDS PAGE Gel for Western Blotting | 14 |
| Figure 12: Morphology of Halpoid1 KO #1 Cell Line | 16 |
| Figure 13: Immunoblot analysis of RACK1 | 18 |
| Figure 14: Analysis of Viral IRES Translation of FLAG and SNAP Fusion Proteins | 20 |
| Figure 15: Analysis of Viral IRES Translation of ybbr Fusion Protein | 22 |
| Figure 16: Analysis of Cellular IRES Translation of FLAG and SNAP Fusion Proteins | 24 |
| Figure 17: Analysis of Cellular IRES Translation of ybbr Fusion Protein | 26 |

List of Tables

| | |
|------------------------------------------------------------------------|----------|
| Table 1: Initiation Factors for Viral IRES-dependent Translation | 4 |
|------------------------------------------------------------------------|----------|

List of Appendices

| | |
|----------------------------------------------------------|-----------|
| Appendix 1: Dual-Luciferase Values of Viral IRES | 36 |
| Appendix 2: Dual-Luciferase Values of Cellular IRES..... | 38 |

1. Introduction

1.1 Canonical Cap-dependent Translation in Eukaryotes

For protein synthesis to occur, each mature eukaryotic messenger RNA (mRNA) must contain the following elements before leaving the nucleus. The beginning of the mRNA, the 5' end, comprises a modified 7-methylguanosine (m^7G) cap structure also known as the 5' cap. A start and stop codon to signal the ribosome where to begin and terminate translation (not shown). Downstream of the 5' cap is a 5' untranslated region (5' UTR), a coding sequence, and a 3' untranslated region (3' UTR) which includes a polyadenylated tail¹ at the end as shown in figure 1.

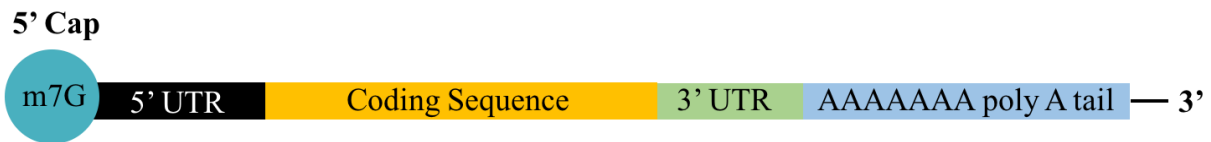


Figure 1: Cartoon structure of a mature mRNA. RNA features pointed out are the 5' cap (m^7G), 5' UTR (black bar), a coding sequence (orange bar), 3'UTR (green bar), and the poly A tail (blue bar).

Canonical translation initiation in eukaryotes begins with the recognition of the mRNA 5' cap by the eukaryotic translation initiation factor 4E (eIF4E) also known as the cap binding protein². Through interactions of eIF4E and other eukaryotic translation initiation factors the linear mRNA strand can circularize. Then the 40S ribosomal subunit is recruited to the 5' end of the mRNA (figure 2). This mechanism is called cap-dependent translation.

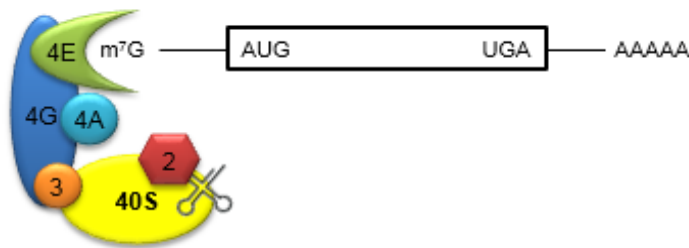


Figure 2: Initiation factors required for cap-dependent translation bound to the mature mRNA linear strand. The cap binding protein eIF4E (green) binds the m⁷G cap of the mRNA. Other translation initiation factors interacting with eIF4E and each other recruit the 40S ribosomal subunit to the 5' end of the mature mRNA. The 40S subunit of the ribosome scans the 5'UTR with the help of the helicase eIF4A (light blue) and starts translation at the start codon AUG.

1.2 IRES-dependent Translation in Eukaryotes

In addition to the cap-dependent translation initiation pathway, specific mRNAs use an internal ribosome entry site (IRESs) to facilitate cap-independent translation initiation or IRES-dependent translation. IRESs are mRNA secondary structures located downstream of the 5' cap commonly in the 5' UTR of viral and cellular mRNAs displayed in figure 3.

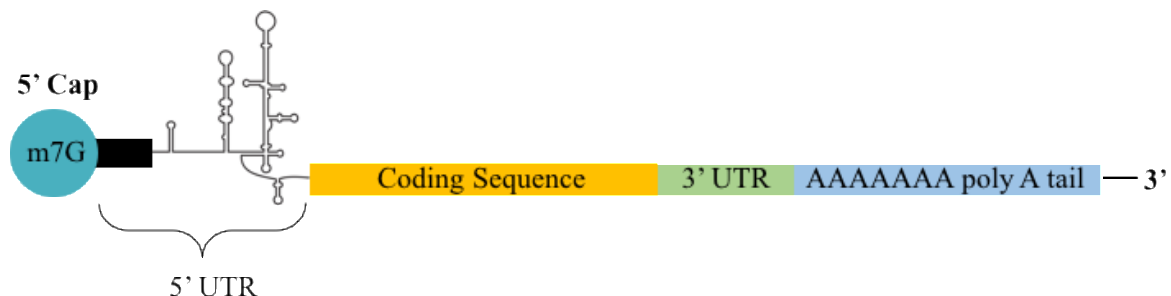


Figure 3: Cartoon structure of an IRES-containing mRNA. Highlighted are the 5'cap (m⁷G), an internal ribosome entry site (IRES) within the 5' UTR, a coding sequence (orange bar), the 3'UTR (green bar), and the poly A tail (blue bar).

IRESs are able to initiate translation using fewer initiation factors than cap-dependent translation (figure 4), and hence allow for translation of mRNAs when translation initiation is

impaired. Specifically, under conditions of cellular stress eIF2 α becomes phosphorylated, which brings translation to a halt³. During poliovirus infection, eIF4G, a scaffolding protein that bridges the interaction of the mRNA 5' and 3'ends via eIF4E and polyA binding protein (PABP) is cleaved⁴. Loss of eIF4G inhibits cellular cap-dependent protein biosynthesis, but allows for translation of specific mRNAs using non-canonical IRES-dependent translation pathways⁵. Since IRES-dependent translation is upregulated during viral infection for this reason, IRESs have become an appealing target for therapeutics⁵.

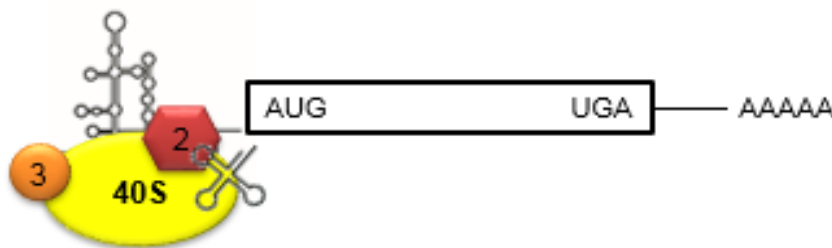


Figure 4: Initiation factors required for HCV IRES-dependent translation. The 40S ribosomal subunit directly binds to the start codon with eIF2 and eIF3.

1.3 The Classes and Functions of the IRES

IRESs are organized into four different types according to their secondary structure, complexity of initiation mechanism, and if the ribosome is recruited upstream of the start codon or directly at it^{1,6}. The specific folds of the IRES are strategic in order to recruit the translation machinery, the ribosome, to the viral genome. Class I and II IRESs require the most components such as cellular auxiliary factors and eukaryotic initiation factors (eIFs) for the proper assembly of the ribosome. Class III requires a limited set of eIFs and Class IV is the most compact and can begin translation without any initiation factors⁷. The two IRESs illustrated in this study are by the cricket paralysis virus (CrPV) and hepatitis C virus (HCV) IRES which are Class IV and III⁸ respectively. Within each IRES are domains that are able to form high-affinity complexes with

the 40S ribosomal subunit¹. Below is a table of required initiation factors for IRES-dependent translation (table 1).

Table 1: Eukaryotic Initiation factors required for IRES-dependent translation within each class for CrPV, HCV, EMCV, and PV.

| Virus | Class of IRES | Initiation Factors Needed |
|-----------------------------------|---------------|--------------------------------------------------------|
| Cricket Paralysis Virus (CrPV) | IV | NONE |
| Hepatitis C Virus (HCV) | III | (eIF2A, eIF2D), eIF2, eIF3, and eIF5 |
| Encephalomyocarditis Virus (EMCV) | II | eIF1A, eIF1, eIF2, eIF3, eIF4A, eIF4B, eIF4G-Ct |
| Polio Virus (PV) | I | eIF1, eIF1A, eIF2, eIF3, eIF4A, eIF4B, eIF4G-Ct, PCBP2 |

1.4 The Presence of two IRESs in Cricket Paralysis Virus

Since the components of protein biosynthesis are not encoded in the genomes of viruses, they must use an alternative pathway for translating their genome. The cricket paralysis virus (CrPV) belongs to the *Dicistroviridae* family and contains a positive-sense RNA genome of approximately 8500-10000 nucleotides in length. As the name *Dicistroviridae* indicates, viruses that belong to this family contain two open reading frames (ORFs). Translation of each ORF is controlled via an IRES, which is termed the 5' UTR IRES and the intergenic region (IGR) IRES. The 5' UTR IRES directs translation of non-structural protein whereas the CrPV_{IGR} IRES directs translation of structural proteins. The CrPV_{IGR} IRES is a 190 nucleotides segment with three domains and has been very well studied which is depicted in figure 5. It represents the most extreme form of an IRES because it does not use any initiation factors to initiate translation¹.

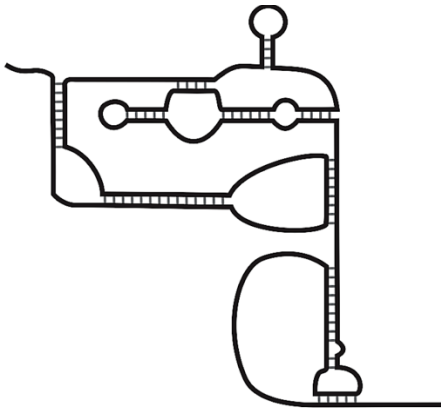


Figure 5: The 190 nucleotide long intergenic cricket paralysis virus (CrPV) IRES which does not require any initiation factors.

The 5' IRES is less well studied however it was found that eIF1, eIF2, and eIF3 are required for this specific IRES-dependent translation⁹. In this thesis, we will utilize the intergenic IRES which requires no initiation factors.

1.5 The Role of the 5' IRES in Hepatitis C Virus Infection

The hepatitis C virus (HCV) genome is a positive-sense single-stranded RNA and is about 9600 nucleotides long¹⁰. HCV is a member of the *Flaviviridae* family and is the foremost cause of liver disease and hepatocellular carcinoma¹¹. Within the 5' UTR, the HCV RNA contains an IRES element, which is used to mediate translation (figure 6).

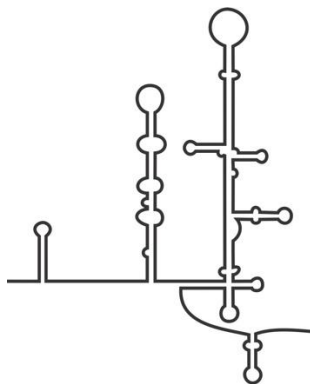


Figure 6: Depiction of the hepatitis C virus IRES within the 5' untranslated region of the 9,600 nucleotide long genomic RNA without initiation factors shown.

In the case of HCV, the IRES can directly recruit the 40S ribosomal subunit to the start codon to initiate protein synthesis. In contrast to the CrPV_{IGR} IRES, the HCV IRES requires translation initiation factor eIF3. The binding of eIF3 to the IRES allows for further initiation factors to bind and inevitably, the 40S subunit¹. In addition to eIF3, which is thought to act as a scaffolding complex¹², eIF2 brings the initiator tRNA to the start codon and GTP hydrolysis by eIF5 allows for binding of the 60S ribosomal subunit¹³ (as illustrated in figure 4).

1.6 The Role of the 5' Polio Virus IRES

Part of the *Picornaviridae* virus family, poliovirus (PV) is a positive-sense stranded¹⁴ RNA that is 7,433 nucleotides long and is covalently linked to a small protein (VPg) at the beginning of the RNA. The poliovirus IRES is composed of nucleotide 124-630 and has 5 complex stem loop structures¹⁵ showed below in figure 7.

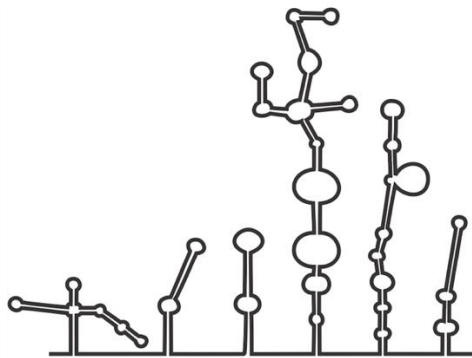


Figure 7: The class (IV) structured poliovirus IRES is located in the 5' UTR of the 7,433 nucleotide long genome without initiation factors shown.

Poliovirus is highly infectious and can cause lifelong or even deadly muscle paralysis. It was one of the most feared viruses in the United States before the invention of a vaccine in the 1950's. There were over 15,000 reported cases per year of infection before a vaccine was developed¹⁶ which has since almost globally eradicated poliovirus. The attenuated vaccine strains

developed by Albert Sabin for all three serotypes of the poliovirus contains a single point mutation within the IRES¹⁷. This results in a decrease in translation of the uncapped viral genome therefore proving an effective solution¹⁸. Compared to the inactivated poliovirus vaccine developed by Jonas Salk, that is mainly used in developed countries, the Sabin vaccine was essential for poliovirus eradication efforts because of its easy oral delivery in developing countries¹⁹.

1.7 The Role of the 5' Encephalomyocarditis Virus IRES

Another member of the *Picornaviridae* virus family, encephalomyocarditis virus (EMCV) is a virus regarded as a zoonotic pathogen which has infected a broad spectrum of organisms. Among the most known affected are pigs which have been commonly infected with EMCV in swine farms. EMCV induces sudden death in piglets as well as reproductive disorders in pregnant pigs; however the interaction mechanism of the host and the virus is fairly unknown²⁰. EMCV is translationally controlled by an IRES within the 5' UTR of the RNA. The EMCV IRES contains 718 nucleotides²¹ and is shown by the structure below in figure 8.

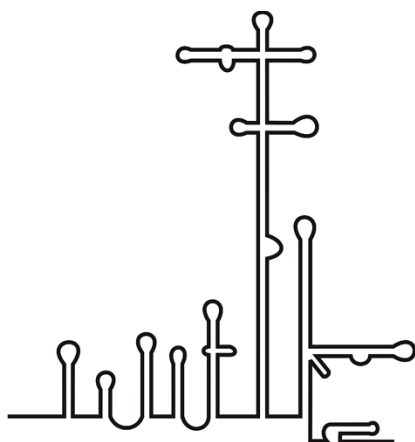


Figure 8: The structure of a class II viral IRES, EMCV, which is part of the *Picornaviridae* family without initiation factors shown.

1.8 The Utilization of Cellular IRES during Stress

Approximately 5 to 10% of cellular mRNAs have been predicted to contain IRES elements in their 5' UTRs. In contrast to the viral genomes discussed above which do not contain a m⁷G cap, cellular IRESs contain a cap²². These particular genes which include IRESs mainly encode proteins regulating growth or cellular differentiation and proteins involved in cellular stress responses⁵. A few of the proposed cellular IRESs selected for our study are myb, Bag-1, c-myc, L-myc, cyclin-D, and Set7. While for most of these cellular IRES, the RNA structure, required factors and detailed mechanism of IRES-dependent translation are poorly understood, the structure of the c-myc IRES has been previously studied. Although the c-myc RNA has an IRES to begin translation internally, protein synthesis can also occur via the canonical mechanism. During times of cellular stress which may result in apoptosis, the cell switches from cap-dependent to the IRES-mediated translation initiation pathway during c-myc protein synthesis²². The structure of the c-myc IRES is indicated below²³.

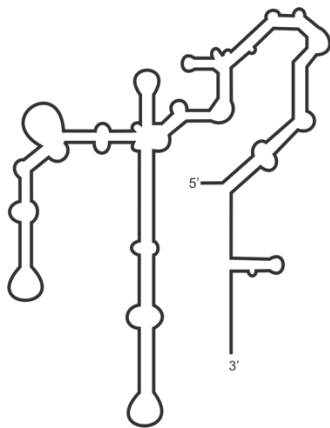


Figure 9: Structure of the cellular IRES, c-myc, indicated by a flexible secondary RNA structure containing bulges and hairpins.

1.9 Ribosomal Filter Hypothesis

Protein biosynthesis is the process of reading an mRNA template and translating the encoded information into a polypeptide sequence. This process is performed by a cellular machinery, the ribosome. Surprisingly, ribosomes are heterogeneous molecules that differ in their composition between tissues or even within the same cell²⁴. Based on this finding, it was suggested that the ribosome itself might be able to regulate protein biosynthesis. This idea is known as the ribosomal filter hypothesis. The ribosome filter hypothesis suggests the following: during translation, ribosomal RNA (rRNA) or ribosomal proteins may interact with mRNAs via mRNA-rRNA base pairing between complementary nucleotide sequences or interactions of mRNAs with ribosomal proteins, respectively. Furthermore, it is thought that these interactions between mRNAs and ribosomes can be rapidly altered in response to changes in the cellular environment or stress allowing cells to rapidly adjust their proteome. By altering ribosome composition, specific mRNAs will be better translated than others²⁵. Evidence supporting this hypothesis comes from recent research, which has shown that eL38 regulates translation of specific HOX genes and eS25 is required for translation of mRNAs that contain an internal ribosome entry site (IRES)^{24,26,11}.

1.10 Ribosome Structure

Eukaryotic ribosomes are composed of two subunits, the small 40S ribosomal subunit, and the large 60S ribosomal subunit. The 40S ribosomal subunit contains the 18S rRNA and about 33 ribosomal proteins; the 60S ribosomal subunit contains the 28S, 5S and 5.8S rRNAs and approximately 46 ribosomal proteins²⁷. Most interactions between mRNA and rRNA are with the

40S subunit, and it is thought that binding of the 40S ribosomal subunit to the mRNA is a rate-limiting step for protein biosynthesis²⁵.

1.11 Ribosomal Protein Receptor for Activated C Kinase 1 (RACK1)

RACK1 is a component of the 40S ribosomal subunit and has a variety of unique functions in the cell. First, RACK1 serves as an adaptor protein, which allows for the interaction of a variety of signaling molecules²⁸. For example, p38 mitogen-activated protein kinase (MAPK) is a molecule that interacts with RACK1 during signaling pathways activated by certain stimuli²⁹. Further, RACK1 has also been shown to integrate the microRNA pathway with ribosomes and translation by its interaction with Ago protein. While it has been shown that RACK1 is not required for 5' cap-dependent translation, RACK1 is required for translation of Drosophila C virus and CrPV¹¹. Specifically, RACK1 is required for translation of the 5' IRES, but not for translation of the CrPV_{IGR} IRES. or translation of Drosophila C virus, Further, it has been also demonstrated to be an essential factor for translation of the HCV IRES and during hepatitis C virus infection¹¹.

1.12 Development of RACK1 fusion proteins to investigate RACK1 function

To investigate protein biosynthesis, single molecule experiments have been proven to be a powerful tool. However, the currently existing tools to study mammalian translation regulation are limited^{30,31}. Thus, fluorescently-labeled RACK1 may allow for its use in single molecule translation experiments. To determine whether RACK1 fusion proteins are functional, RACK1 fusion proteins with four different protein tags, namely FLAG, SNAP and N-terminal and C-terminal ybbr tags, were expressed in the RACK1 KO #1. The FLAG tag is a short peptide sequence of DYKDDDDK commonly used hydrophilic protein. This protein tag allows for elution

under denaturing and non-denaturing conditions and several antibodies against this peptide sequence have been developed³². The SNAP tag is a 20 kDa mutant of the DNA repair protein O⁶-alkylguanine-DNA alkyltransferase. This tag is commonly used for its site-specific coupling of recombinant proteins to surfaces which assures proper labeling³³. Two add-back cell lines were created using the ybbr tag placed at the 5' and the 3' end of the protein. This tag, initially discovered in *Bacillus subtilis*³⁴, is only 11 residues in length with a sequence of DSLEFIASKLA and forms a short alpha-helical structure. The small size, flexibility of tagging location and the choice in fluorophore color has great potential for its use in smFRET experiments³⁵. It is important to choose small protein tags to label our protein of interest so that we do not interfere with the function of the protein itself.

1.13 Goal/Question

Previous research has shown that RACK1 is required for translation of the HCV IRES but not of the CrPV_{IGR} IRES. To determine if RACK1 is generally needed for IRES-mediated translation of viral and cellular RNAs, we performed dual-luciferase reporter assays to measure cap-dependent and IRES-dependent translation in in wildtype haploid 1 (hap1) cells, RACK1 knockout and RACK1 add-back cell lines. In this study, we have not only included the CrPV_{IGR} and HCV IRES as negative and positive control, respectively, we also tested if PV and EMCV, two other viral IRESs, also require RACK1 for efficient IRES-dependent translation. In addition, we also tested if RACK1 is required for translation of six selected cellular IRESs: myb, Bag-1, c-myc, L-myc, cyclin-D, and Set7. While for most of these cellular IRES, the RNA structure, required factors and detailed mechanism of IRES-dependent translation are poorly understood, our

research has elucidated that RACK1 is a conserved factor required for both viral and cellular IRES-dependent translation.

2. Materials & Methods

2.1 Use of a Bicistronic Construct to Test IRESs Activity

To confirm whether RACK1 is required for IRES-dependent translation, we employed a dual-luciferase reporter system using a codon-optimized bicistronic construct that contained a *Renilla* luciferase reporter upstream and a firefly luciferase reporter downstream of a viral or cellular IRES. Shown in figure 10 is the IRES_{HCV}-luciferase reporter construct. Translation of the *Renilla* open reading frame was mediated by canonical cap-dependent translation initiation. In contrast, translation of the firefly luciferase was dependent on a viral or cellular IRES. To account for differences in transfection efficiency, the amount of *Renilla* luciferase produced in cells were used to normalize the IRES activity³⁶. The results are expressed as a ratio of Firefly/*Renilla* (see appendix).

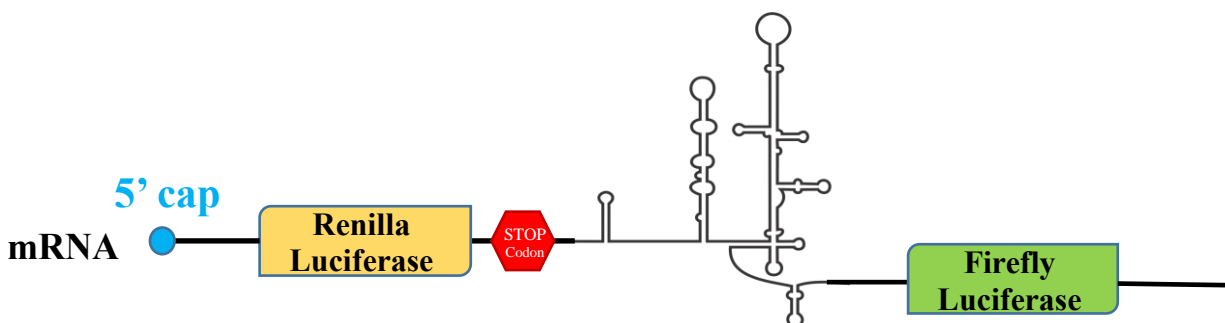


Figure 10: Cartoon structure of the IRES_{HCV}-bicistronic luciferase reporter. *Renilla* luciferase is produced by canonical cap-dependent translation, while the IRES controls translation of the firefly luciferase cistron downstream of the IRES.

2.2 Immunoblot to Detect Knockout Cell Line

RACK1 knockout cells had been generated prior to this thesis³⁷. Two separate knockout clonal cell lines were isolated and will be called KO #1 and KO # 2 for clarity. KO #1 was transduced with lentivirus encoding the RACK1 protein C-terminally fused with the FLAG-tag called RACK-FLAG was the add-back control. To validate the cell lines, cells were harvested in radioimmunoprecipitation assay buffer (RIPA) (1% Nonidet P-40, 0.5% sodium deoxycholate ad

0.1% sodium deoxycholate in PBS containing a protease inhibitor tablet (Roche)). Cleared protein extracts were mixed with 2X Laemmli protein loading buffer (10% SDS, glycerol, 1 M Tris-Cl (ph 6.8), in H₂O, 100 mM DTT) + RIPA buffer by adding 8 μ L of the cell lysate to 12 μ L of 2X SDS loading buffer+DTT. Samples were boiled at 95°C for 10 minutes in a LabNet Digital Heatblock. Samples were spun down and 20 μ L of the protein samples were loaded using a p20 pipette and appropriate tips into each well according to the order in figure 11. Samples were then separated in a 12% SDS Polyacrylamide Gel in 1X Laemmli running buffer (192 mM glycine, 25 mM 6 Tris base, 0.1% SDS).

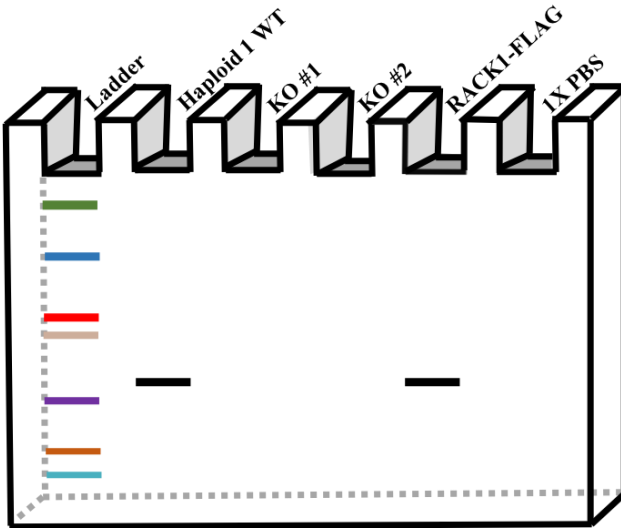


Figure 11: Cartoon depiction of SDS-PAGE gel. From the far left: the molecular weight marker, haploid 1 WT, KO #1, KO #2, RACK1-FLAG and 1X PBS were loaded in a vertical 12% SDS Polyacrylamide gel system. Direction of migration of the samples shown above. For simplification, only the marker bands and the RACK1 bands are shown.

The gel was run at 70V until the bromophenol blue dye entered the resolving gel; voltage was then increased to 120V for approximately 1 hour until bromophenol blue dye had reached the bottom of the gel. Proteins were transferred onto a nitrocellulose membrane (Amersham) via wet transfer at 100V for 1 hour. This was done at 4°C in 1X Transfer buffer (192 mM glycine, 25 mM Tris base, 0.1% SDS, 20% mL methanol).

Following the transfer, the membrane was stained using Ponceau S (Sigma-Aldrich, 0.1 % (w/v) in 5% acetic acid) for 5 minutes then rinsed several times with about 5 mL of PBS-Tween 20 (0.05% pH 7.5) to validate protein transfer. To prevent non-specific binding the membrane was blocked in 5% non-fat milk for 1 hour at room temperature, then rinsed three times in PBS-T to wash away milk remnants.

The membrane was incubated overnight at 4°C in a 1:1000 dilution of RACK1 primary antibody (cell signaling, RACK1 (D59D5) Rabbit mAb #5432) in 5% BSA-PBS/T. After primary incubation, the membrane was washed four times for 15 minutes each in about 10 mL of PBS-T. Next, the membrane was incubated in a 1:10000 dilution of secondary goat anti-rabbit-HRP antibody (Jackson) in 5% milk-PBS-T for 2 hours at room temperature. Following four 15-minute washes with 10 mL of PBS-T the membrane was imaged using standard chemiluminescence solution (Pierce) on a BioRad Chemicdoc gel imager. As a loading control, the membrane was incubated in a 1:1000 dilution of RPS25 primary antibody (abcam, (ab102940)) overnight at 4°C. The procedures described above were repeated to visualize RPS25 signal.

2.3 Seeding Cells

The day prior to transfection, 20,000 cells/well of haploid1 wildtype, RACK1 knockouts, and RACK1 add-back cell lines were seeded into wells of a 96-well plate to reach 70-90% confluence on the day of transfection. Figure 12 illustrates the cell morphology of the KO #1 cell line prior to transfection.

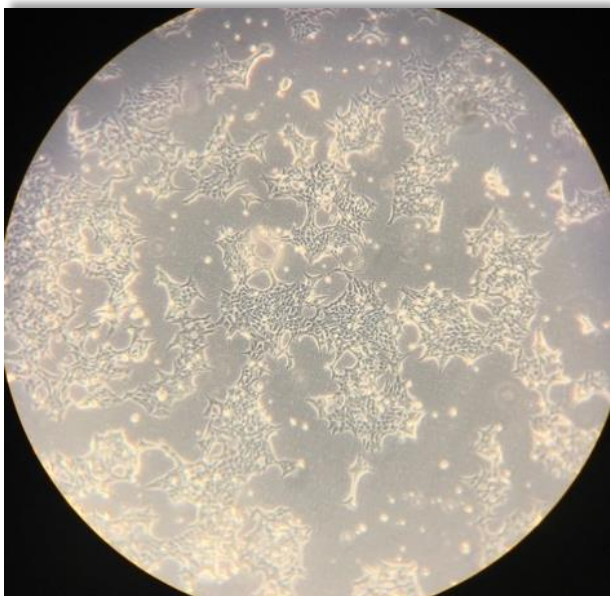


Figure 12: The figure above shows the morphology of RACK1 KO#1 in a 6 cm dish before splitting the cells for transfection.

2.4 Lipofectamine Transfection of IRES-luciferase Reporter Construct

Transfection reactions were completed in a sterile environment to prevent bacterial contaminations. First, the lipid reagent was diluted in 50 μL of transfection media OptiMEM (ThermoFisher Scientific). To transfect one well of a 96-well plate, 0.3 μL Lipofectamine 3000 reagent (ThermoFisher Scientific) was diluted in a microcentrifuge tube into 5 μL of OptiMEM. In a second microcentrifuge tube, 0.1 μg plasmid DNA of the bicistronic luciferase reporter and 0.2 μL P3000 reagent were also diluted in 5 μL of OptiMEM. Next, the lipofectamine dilution was added to the diluted DNA (1:1 ratio), mixed and briefly spun down in a microcentrifuge. Reactions were incubated for 10 minutes at room temperature. Lastly, 10 μL of the DNA-lipid complex was added to one well of cells. Cells were incubated for 24 hours at 37°C, 5% CO_2 in a tissue culture incubator. For multiple transfections, the reactions were scaled up accordingly.

2.5 Reading *Renilla* and Firefly Luciferase Signal

Following aspiration of cell media, cells were lysed by addition of 20 μ L of 1X Passive Lysis buffer (PLB) to each well. Firefly and *Renilla* luminescence of 20 μ L of cell lysates were measured with a GloMax 20/20 luminometer (Promega) in a white, flat-bottom 96-well plate using luciferase assay and Stop & Glo reagents (Promega). Following luminescence measurement, the Firefly/*Renilla* signal intensity was calculated. The average of at least three biological replicates was plotted. Error bars represent the standard error of the mean (SEM) and asterisks represent the p-values for each cell line.

3. Results

3.1 Immunoblot of RACK1 WT, RACK1 Knockouts, and RACK1 Add-back Cell Lines

Lack of RACK1 protein in the two RACK1 knockout cell lines (KO #1 and KO #2) was validated by immunoblotting. The immunoblot figure 13 shows that RACK1 is present in both the RACK1 WT and RACK-FLAG cell lines. No signals were detected in both KO #1 and KO #2 indicating that RACK1 is absent in these cell lines. These cell lines were then used in our transfection to test the effect of RACK1 during IRES-dependent translation.

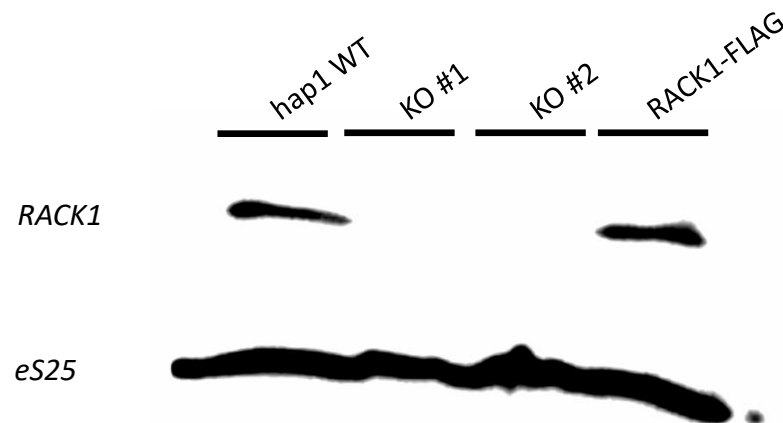


Figure 13: Immunoblot analysis of RACK1. The above figure shows the presence of two RACK1 knockouts and the presence of RACK1 in the hap1 WT and RACK-FLAG cell lines indicated by a band. A Western Blot was performed which probed with RACK1 antibody in RACK1 WT, RACK1 KO's and RACK-FLAG cell lines. The blot was then probed with RPS25 antibody as a loading control to show equal protein loading.

3.2 Viral IRES-dependent Activity in Hap1 WT, KO #1, KO #2, RACK1-FLAG and RACK1-

SNAP

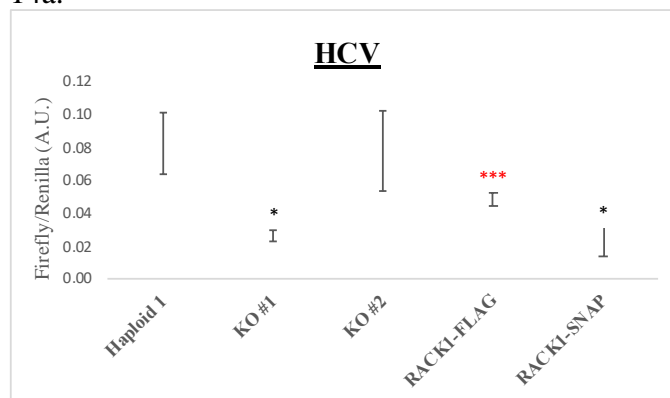
Using a dual-luciferase assay we tested whether RACK1 is required for four structurally and functionally different viral IRESs. Since it had been previously shown that CrPV_{IGR} IRES does not require RACK1 for translation, this construct served as a negative control¹¹. In agreement with

previous findings by Mazjoub et al., the CrPV_{IGR} IRES remains unchanged in the absence of RACK1 compared to WT levels (figure 14b).

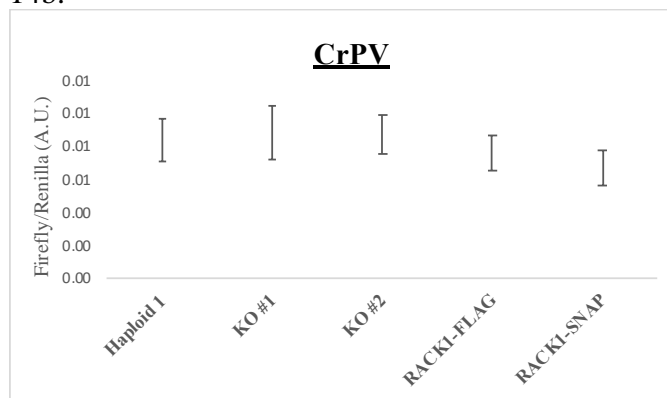
The HCV IRES differs from the CrPV IRES and was previously shown to require RACK1 for translation¹¹. Compared to wildtype cells RACK1 knockout cell lines showed a decrease in the Firefly/*Renilla* ratio, with only statistical significance in KO #1, indicating that IRES activity was decreased in the RACK1 knockout cells. When RACK1 was expressed in the RACK1 FLAG and SNAP tags, IRES activity was fully recovered in RACK1-FLAG, however not recovered in RACK1-SNAP (figure 14a).

In addition to these two previously tested IRESs, we also measured if RACK1 was required for translation of two other viral IRESs, specifically the EMCV and PV IRES. Similar to the HCV IRES, the EMCV and PV IRESs show high activity in the haploid1 wildtype cell line. In cells lacking RACK1, the Firefly/*Renilla* ratio was significantly decreased in both (figure 14c and 14d). Although we observed partial rescue in most add-back cell lines, the RACK-FLAG cell line rescued almost to wildtype levels (figure 14c) for the EMCV IRES however failed to rescue in PV (figure 14d). The RACK1-SNAP tag was insufficient in rescuing to statistically significant values in the HCV, EMCV, and PV IRESs.

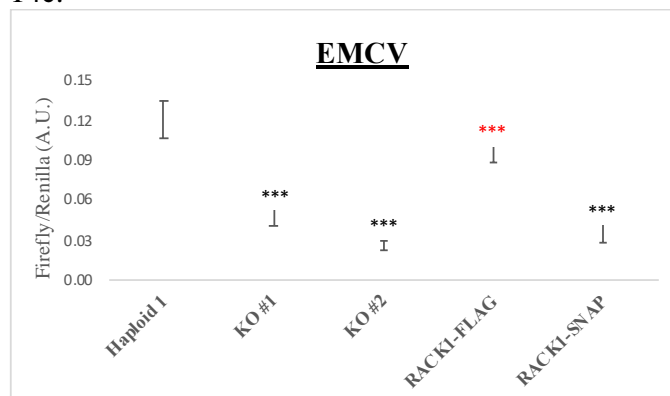
14a.



14b.



14c.



14d.

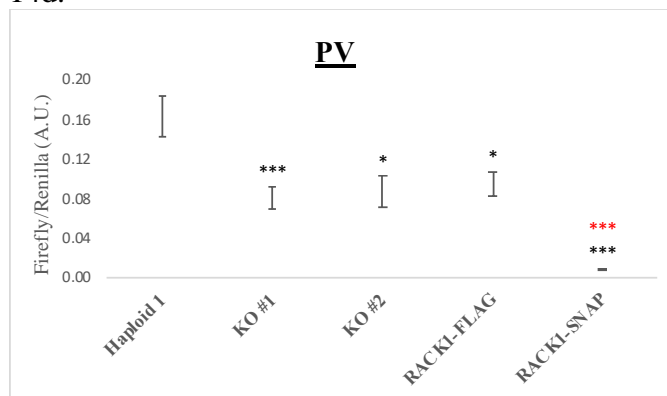


Figure 14 a-d: Analysis of viral IRES-mediated translation using bicistronic luciferase constructs with FLAG and SNAP RACK1 fusion proteins. HCV, EMCV, and PV viral IRES show decrease with mostly statistical significance of cells lacking RACK1 compared to the haploid1 WT cells. There is partial recovery in RACK1-FLAG cells and insufficient recovery in the RACK1-SNAP tag. Dual-luciferase plasmid DNA was transfected into WT, RACK1 KO and RACK1 add-back cell lines. Twenty-four hours post transfection, cells were harvested, and *Renilla* and *Firefly* levels was measured with a luminometer. Plotted are the averages of at least three independent experiments. Error bars represent the standard error of the mean (SEM) and asterisks represent the p-values for each cell line. Black asterisks denote levels compared to haploid1 and red asterisk denote levels compared to KO #1.

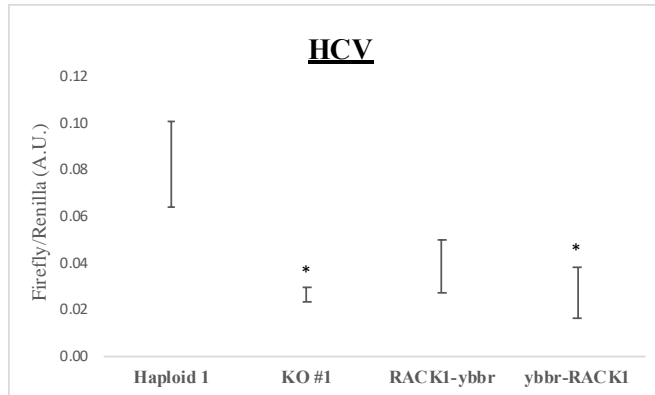
3.3 Viral IRES-dependent Activity in Hap1 WT, KO #1, RACK1-ybbr and ybbr-RACK1

The ybbr tags were used due to the small size of the tag limiting the chance of interference of the protein of interest. This tag was added to either the 5' or the 3' end and is labeled ybbr-RACK1 and RACK1-ybbr respectively. The RACK1 KO #1 was used to compare levels of the ybbr add-back cell lines because this specific KO had been the transduced. Each tested viral IRES was efficiently translated in haploid1 WT cells and decreased in the knockout cell lines. Although

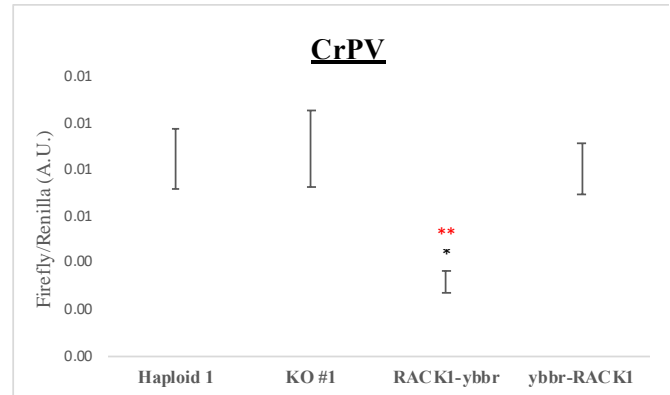
the ybbr tags seem to pose as effective tags in theory, they did not recover with statistical significance in each case compared to KO #1.

In Figure 15a and 15c show very similar trends of the HCV and the EMCV IRESs. Firefly/*Renilla* luciferase ratios were high in haploid1 cells and decreased in the KO #1 with statistical significance; however the 5' and 3' terminal ybbr fusion proteins did not recover well. Similar to the HCV and EMCV viral IRES, the PV IRES shows a decrease in the ratio of Firefly/*Renilla* without statistical significance. Both ybbr tags did not recover and it is noticed that the levels of RACK1-ybbr are lower than the KO #1 (figure 15d). Since RACK1 is not required for translation of CrPV, we should expect to see unchanging levels from the haploid1 cell line, however there was a decrease *Renilla* value causing a decrease in the ratio in RACK1-ybbr.

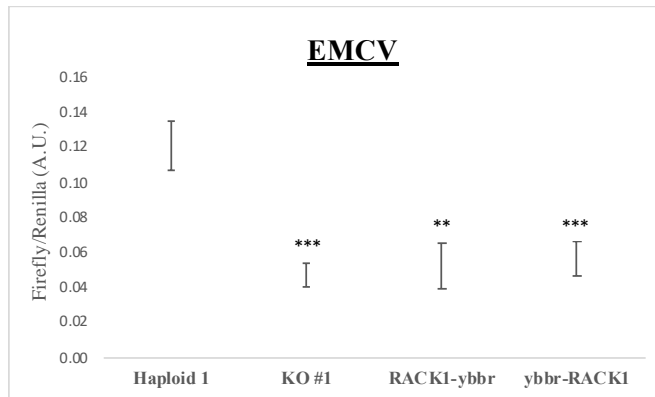
15a.



15b.



15c.



15d.

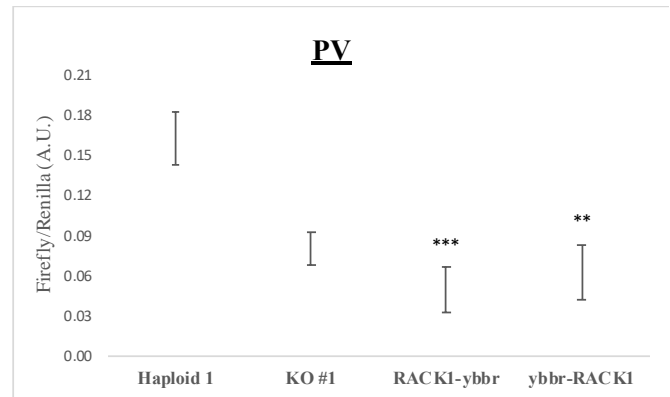


Figure 15 a-d: Analysis of viral IRES-mediated translation using bicistronic luciferase constructs with ybbr RACK1 fusion proteins. HCV, EMCV, and PV viral IRES show decrease with mostly statistical significance of cells lacking RACK1 compared to the haploid1 WT cells. There is insufficient recovery in both the RACK1-ybbr and ybbr-RACK1 tags. CrPV IRES level activity remains constant except for decreased levels in RACK1-ybbr. Dual-luciferase plasmid DNA was transfected into WT, RACK1 KOs and RACK1 add-back cell lines. Twenty-four hours post transfection, cells were harvested, and *Renilla* and *Firefly* levels was measured with a luminometer. Plotted are the averages of at least three independent experiments. Error bars represent the standard error of the mean (SEM) and asterisks represent the p-values for each cell line. Black asterisks denote levels compared to haploid1 and red asterisk denote levels compared to KO #1.

3.4 Cellular IRES-dependent Activity in Hap1 WT, KO #1, KO #2, RACK1-FLAG and

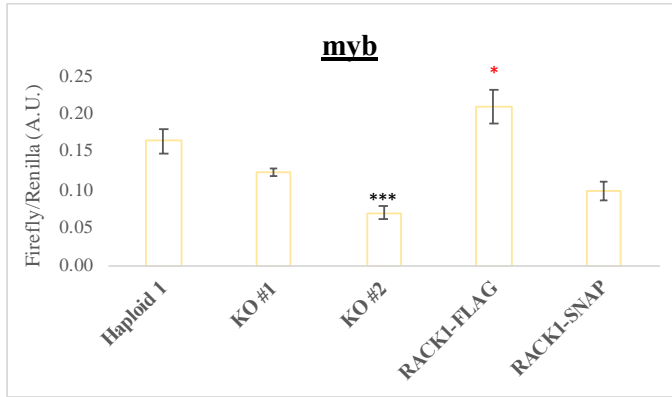
RACK1-SNAP

In addition to viral IRESs, certain cellular mRNAs have been shown to contain an IRES to ensure translation of these mRNAs under conditions of cellular stress. We wondered whether RACK1 was only required for translation of viral IRESs, or if it may also contribute to translation

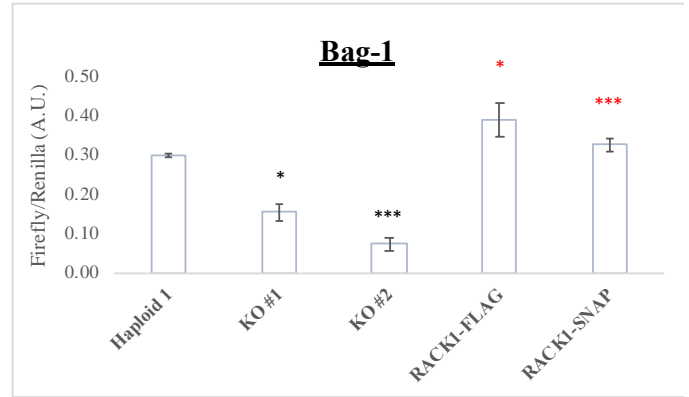
of cellular IRESs. We therefore tested translation of myb, Bag-1, c-myc, L-myc, cyclin D, and Set7 IRESs in the presence and absence of RACK1 which is represented in figure 16.

For myb, Bag-1, cyclinD, and Set7, we observed a similar pattern as already observed for the viral IRESs we had tested. Specifically, we found that these IRESs were well translated in wildtype cells, but that translation was decreased in cells lacking RACK1. RACK1 KO#1 displayed a significant decrease in Bag-1, L-myc, and Set7 IRES translation compared to haploid1 cells. Similarly, every cellular IRES showed a significant decrease in the ratio of Firefly/*Renilla* of KO #2 compared to haploid1 cells. The RACK-FLAG add-back cell line rescued every IRES activity to levels higher than the wildtype cell line. Lastly, the RACK-SNAP add-back rescued translation of Bag-1, c-myc, L-myc, and Set7 IRESs with statistical significance.

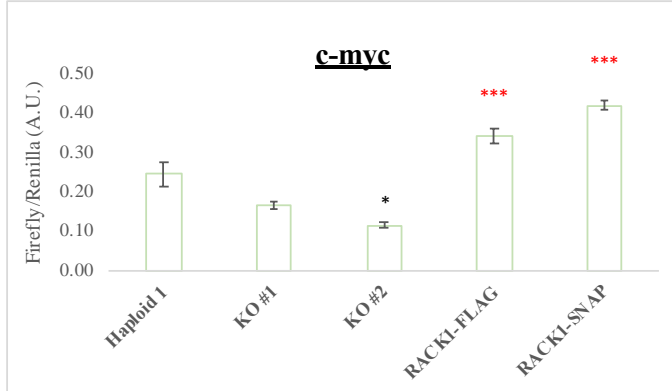
16a.



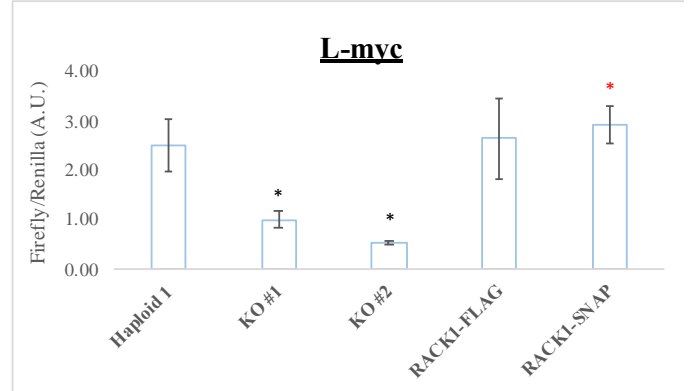
16b.



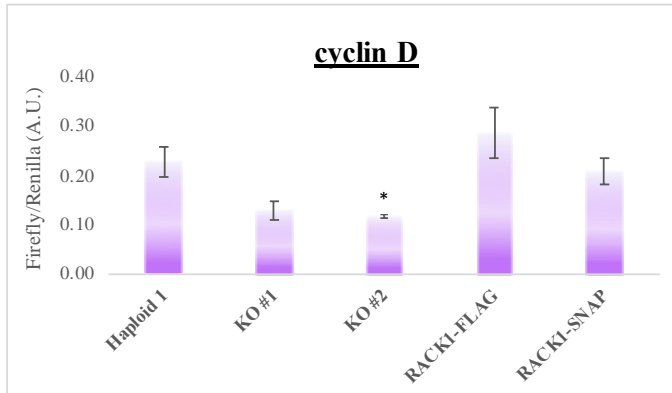
16c.



16d.



16e.



16f.

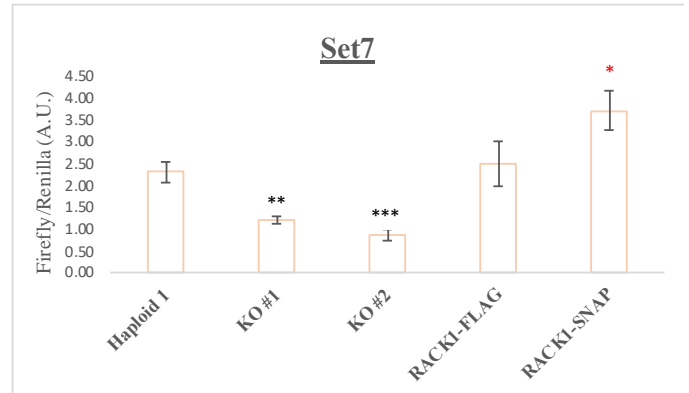


Figure 16 a-f: Analysis of cellular IRES-mediated translation using bicistronic luciferase constructs with FLAG and SNAP RACK1 fusion proteins. Six different cellular IRES show decrease with mostly statistical significance of KO #1 compared to the haploid WT cells. There was recovery in L-myc and Set7 of RACK1-ybbr compared to KO #1 with no recovery in the rest. Lastly, the ybbr-RACK1 add-back rescued translation of all cellular IRESs with statistical significance in on Bag-1, c-myc, cyclin D, and Set7 with significance. Dual-luciferase plasmid DNA was transfected into WT, RACK1 KOs and RACK1 add-back cell lines. Twenty-four hours post transfection, cells were harvested, and *Renilla* and Firefly levels was measured with a luminometer. Plotted are the averages of at least three independent experiments. Error bars represent the standard error of the mean (SEM) and asterisks represent the p-values for each cell line. Black asterisks denote levels compared to haploid1 and red asterisk denote levels compared to KO #1.

3.5 Cellular IRES-dependent Activity in Hap1 WT, KO #1, RACK1-ybbr and ybbr-RACK1

Using similar logic in section 3.3, cellular IRESs were tested in the ybbr-tag expressing add-back cell lines. As previously discussed, all translation of all cellular IRESs is reduced in the haploid cells, but translation of Bag-1, L-myc, and Set7 IRESs was significantly reduced in RACK1 KO#1 cells compared to hap1 WT cells. For the cellular IRES constructs, ybbr-RACK1 expression significantly rescued translation of the L-myc and Set7 IRESs. For the other IRES constructs myb, Bag-1, c-myc and cyclin D, translation was rescued, but not statistically significant when compared to KO #1. The rescue for the ybbr-RACK1 expressing add-back cell line was better compared to RACK1-ybbr showing statistical significance for Bag-1, c-myc, cyclin D and Set7 IRES. The myb and L-myc cellular IRES were able to rescue the IRES translation deficit of the KO #1, but the rescue was not statistically significant. See figure 17 below.

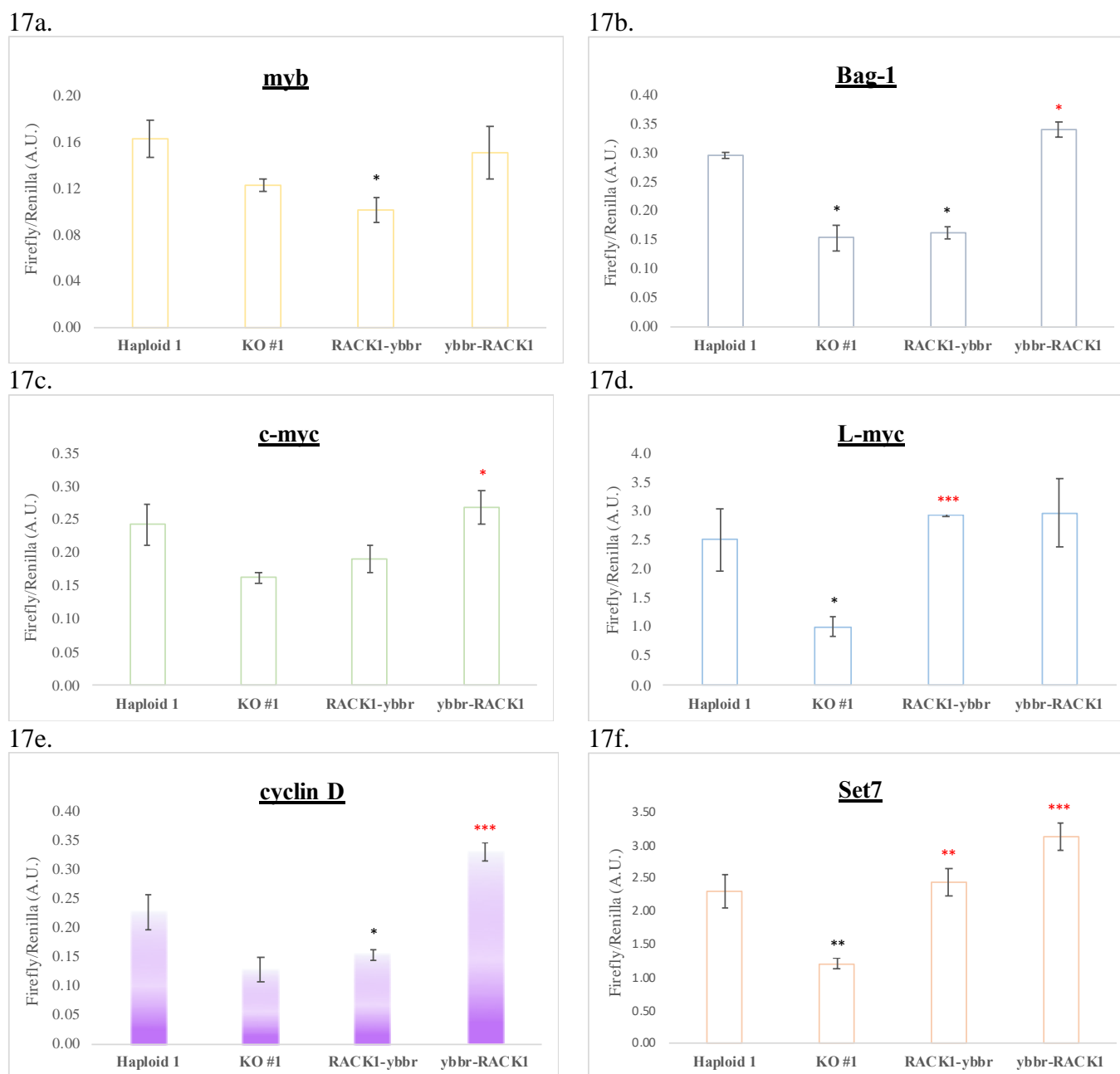


Figure 17 a-f: Analysis of cellular IRES-mediated translation using bicistronic luciferase constructs with ybbR RACK1 fusion proteins. Six different cellular IRES show decrease with mostly statistical significance of KO #1 compared to the haploid1 WT cells. There was recovery in L-myc and Set7 of RACK-ybbr compared to KO #1 with no recovery in the rest. Lastly, the ybbr-RACK1 add-back rescued translation of all cellular IRESs with statistical significance in only Bag-1, c-myc, cyclin D, and Set7 with significance. Dual-luciferase plasmid DNA was transfected into WT, RACK1 KO, and RACK1 add-back cell lines. Twenty-four hours post-transfection, cells were harvested, and *Renilla* and Firefly levels were measured with a luminometer. Plotted are the averages of at least three independent experiments. Error bars represent the standard error of the mean (SEM) and asterisks represent the p-values for each cell line. Black asterisks denote levels compared to Haploid1 and red asterisks denote levels compared to KO #1.

4. Discussion

It was recently shown that certain ribosomal proteins are required for translation of specific mRNAs. Ribosomal protein eS25 was shown to facilitate translation of both viral and cellular IRESs. Since RACK1 had been shown to be required for translation of the 5' CrPV_{IRG} IRES and HCV IRES, here we tested whether RACK1 was generally required for translation of IRES-containing mRNAs. Indeed, we found that RACK1 plays a major role in regulating IRES-dependent translation. Using both viral and cellular IRES constructs we conducted dual-luciferase assays in haploid1 wildtype, two different RACK1 knockout cell lines, and RACK1 add-back cell lines. As a positive control, we used the HCV IRES construct because RACK1 had been previously shown to regulate translation of the HCV IRES¹¹. In addition, we verified that RACK1 did not affect the CrPV IRES, which has also been previously reported¹¹.

EMCV and PV IRESs had never been tested as to the role RACK1 plays in translation of these viral IRESs. Utilizing the dual-luciferase assay, we found that RACK1 was needed for both types of IRESs to begin translation. For both IRESs, we observed a significant decrease in translation in the RACK1 knockout cell lines. The RACK1-SNAP, ybbr-RACK1, and RACK-ybbr did not have significant rescue in EMCV as well as all of the add-back cells lines tested with PV. It cannot be excluded that the protein tags interfere with translation of the EMCV and PV IRESs by inhibiting necessary IRES binding, binding of other proteins or a conformational change in the IRES structure. However, due to the lack of structural information of 40S:EMCV IRES or 40S:PV IRES complexes we are unable to test this hypothesis¹³. Translation levels remain fairly constant in each cell line testing the CrPV IRES except for RACK1-ybbr. Since RACK1 is not required for CrPV_{IGR} IRES translation, it is possible that the ribosome binding site for RACK1-ybbr overlaps

with the CrPV IRES, preventing its translation. Alternatively, dual luciferase assays are not always reliable, and it cannot be excluded that the observation cannot be repeated.

We also extended our study by testing the RACK1 requirement for translation of cellular mRNAs containing IRESs. Because cellular IRES-containing mRNAs have a cap and an IRES, it is thought that the IRESs are used for translation initiation when cap-dependent translation is downregulated, for example under conditions of stress. We have shown that RACK1 is required for translation of each cellular IRES with a significant decrease in translation in either the KO #1 or KO #2. Overall, the FLAG tag rescues IRES translation of cellular IRESs better than the SNAP tag, which only showed partial rescue for myb and cyclin D IRESs. In contrast to the viral IRESs, there was significant translation recovery in either the 5' or 3' terminally labeled ybbr tags for each cellular IRES, with the exception of myb and Bag-1. We speculate that the tags added to RACK1 may have led to improper conformational changes similar to our results for the PV IRES. For none of the cellular IRESs, a structure of the 40S:IRES complex is known, so structural studies are not available to shed light into the mechanism of RACK1 in IRES-dependent translation.

All the viral IRESs tested, with the exception of CrPV IRES, require the initiation factors eIF2 and eIF3. Based on the 40S:HCV structure, RACK1 and the HCV IRES are far apart¹³, and it is unlikely that RACK1 directly mediates IRES-dependent translation. A recent structure of the 43S preinitiation complex shows that eIF3d interacts with RACK1¹⁴. We speculate that eIF3 indirectly regulates IRES-dependent translation by bridging the interaction of the IRES with RACK1. Further testing would be required to test if all IRESs that rely on RACK1 also require eIF3d for IRES-dependent translation¹³.

5. Conclusion

First, we confirmed of the loss of RACK1 protein in the RACK1 knockout cell lines. Previously published results showed that RACK1 is needed for HCV IRES-dependent translation but not for CrPV_{IGR} IRES. In agreement with these previous publications, we established that RACK1 is indeed needed for translation of the HCV IRES, but is also required for translation of EMCV, PV and all six tested cellular IRESs. We further confirmed that RACK1 is not required for translation of the CrPV_{IGR} IRES. Expression of tagged-RACK1 is tolerated for certain IRESs, such as HCV, but may interfere with IRES function as seen in PV, myb, Bag-1 c-myc and L-myc and cyclin D.

6. Future Implications

Our luciferase data display some unexpected variation in the rescue of the RACK1 phenotype with different protein tags. An increase in the number of dual-luciferase assays could result in smaller error bars and more robust experimental conclusions.

To further investigate the role that RACK1 plays during viral infection and cellular stress we can extend our studies to methods such as ribosome profiling, RNA and ribosome sequencing, and virus plaque assays to. Ribosome profiling, RNA and ribosome sequencing can help us to identify how loss of RACK1 alters global and gene-specific translation, respectively.

The bicistronic luciferase assays performed and described in this thesis are artificial assays, meaning they do not occur *in vivo*. To investigate the role of RACK1 in cells, haploid cells can be infected with virus. For PV, plaque assays represent an easy and fast measure of how the protein affects virus output. Specifically, poliovirus stock is diluted and used to infect a monolayer of cells. Following the infection, a media-agar layer is added, which allows for infection of only the neighboring cells which appear as plaques at the end of the assay. If RACK1 affects how well the virus can establish an infection, we would observe a decrease in the number of plaques. If loss of RACK1 extends the virus life cycle, we would expect to see smaller poliovirus plaques at the end of the assay.

Overall, our study showed that RACK1 is required for the translation of several viral IRESs. Thus, targeting RACK1 could be a strategy to develop a novel antiviral therapy in the future.

7. References

1. Johnson, A. G., Grosely, R., Petrov, A. N., Puglisi, J. D. & Puglisi, J. D. Dynamics of IRES-mediated translation. (2017). doi:10.1098/rstb.2016.0177
2. Edgil, D., Polacek, C. & Harris, E. Dengue virus utilizes a novel strategy for translation initiation when cap-dependent translation is inhibited. *J. Virol.* **80**, 2976–86 (2006).
3. Roth, H. *et al.* Flavivirus infection uncouples translation suppression from cellular stress responses. *MBio* (2017). doi:10.1128/mBio.02150-16
4. Rivera, C. I. & Lloyd, R. E. Modulation of enteroviral proteinase cleavage of poly(A)-binding protein (PABP) by conformation and PABP-associated factors. *Virology* (2008). doi:10.1016/j.virol.2008.02.002
5. Hertz, M. I., Landry, D. M., Willis, A. E., Luo, G. & Thompson, S. R. Ribosomal Protein S25 Dependency Reveals a Common Mechanism for Diverse Internal Ribosome Entry Sites and Ribosome Shunting. *Mol. Cell. Biol.* **33**, 1016–1026 (2013).
6. Bugaud, O. *et al.* Kinetics of CrPV and HCV IRES-mediated eukaryotic translation using single molecule fluorescence microscopy. *Rna* rna.061523.117 (2017). doi:10.1261/rna.061523.117
7. Mailliot, J. & Martin, F. Viral internal ribosomal entry sites: four classes for one goal. *Wiley Interdisciplinary Reviews: RNA* (2018). doi:10.1002/wrna.1458
8. Lemon, S. M. & Honda, M. Internal ribosome entry sites within the RNA genomes of hepatitis C virus and other flaviviruses. *Seminars in Virology* (1997). doi:10.1006/smv.1997.0129

9. Terenin, I. M. *et al.* A Cross-Kingdom Internal Ribosome Entry Site Reveals a Simplified Mode of Internal Ribosome Entry. *Mol. Cell. Biol.* (2005).
doi:10.1128/MCB.25.17.7879-7888.2005
10. Boehringer, D., Thermann, R., Ostareck-Lederer, A., Lewis, J. D. & Stark, H. Structure of the hepatitis C virus IRES bound to the human 80S ribosome: Remodeling of the HCV IRES. *Structure* **13**, 1695–1706 (2005).
11. Majzoub, K. *et al.* RACK1 controls IRES-mediated translation of viruses. *Cell* **159**, 1086–1095 (2015).
12. Hinnebusch, A. G. eIF3: a versatile scaffold for translation initiation complexes. *Trends in Biochemical Sciences* (2006). doi:10.1016/j.tibs.2006.08.005
13. Kai Ying Lin, Nabanita Nag, Tatyana V. Pestova, and A. M. Human eIF5 and eIF1A Compete for Binding to eIF5B. *Biochemistry* **57**, 5910–5920 (2018).
14. Semler, B. L. Poliovirus proves IRES-istible in vivo. *Journal of Clinical Investigation* (2004). doi:10.1172/JCI200422139
15. Murray, K. E., Steil, B. P., Roberts, A. W. & Barton, D. J. Replication of Poliovirus RNA with Complete Internal Ribosome Entry Site Deletions. *J. Virol.* (2004).
doi:10.1128/JVI.78.3.1393-1402.2004
16. Okayasu, H., Sein, C., Hamidi, A., Bakker, W. A. M. & Sutter, R. W. Development of inactivated poliovirus vaccine from Sabin strains: A progress report. *Biologicals* (2016). doi:10.1016/j.biologicals.2016.08.005

17. Malnou, C. E., Poyry, T. A. A., Jackson, R. J. & Kean, K. M. Poliovirus Internal Ribosome Entry Segment Structure Alterations That Specifically Affect Function in Neuronal Cells: Molecular Genetic Analysis. *J. Virol.* (2002).
doi:10.1128/JVI.76.21.10617-10626.2002
18. Avanzino BC, Jue H, Miller CM, Cheung E, Fuchs G3, F. C. Molecular mechanism of poliovirus Sabin vaccine strain attenuation. *Biol. Chem.* **293**, 15471–15482 (2018).
19. Lahariya, C. Global eradication of polio: The case for ‘finishing the job’. *Bulletin of the World Health Organization* (2007). doi:10.2471/BLT.06.037457
20. Jia Wei, Haixia Zhang, Xiangrong Li, Qiongyi Li, Zhongren Ma, Jialin Bai, Zilin Qiao, and R. F. Transcriptional profiling of host cell responses to encephalomyocarditis virus (EMCV). *Virology* **14**, (2017).
21. Jang, S. K. *et al.* A Segment of the 5' Nontranslated Region of Encephalomyocarditis Virus RNA Directs Internal Entry of Ribosomes during In Vitro Translation. *Journjal Virol.* (1988). doi:10.1196/annals.1307.020
22. Stoneley, M. & Willis, A. E. Cellular internal ribosome entry segments: Structures, trans-acting factors and regulation of gene expression. *Oncogene* (2004).
doi:10.1038/sj.onc.1207551
23. Le Quesne, J. P. C., Stoneley, M., Fraser, G. A. & Willis, A. E. Derivation of a structural model for the c-myc IRES. *J. Mol. Biol.* (2001). doi:10.1006/jmbi.2001.4745
24. Xue, S. & Barna, M. Specialized ribosomes: A new frontier in gene regulation and organismal biology. *Nature Reviews Molecular Cell Biology* **13**, 355–369 (2012).

25. Mauro, V. P. & Edelman, G. M. The ribosome filter redux. *Cell Cycle* **6**, 2246–2251 (2007).
26. Kondrashov, N. *et al.* Ribosome-mediated specificity in Hox mRNA translation and vertebrate tissue patterning. *Cell* **145**, 383–397 (2011).
27. Wilson, D. N. & Cate, J. H. D. The structure and function of the eukaryotic ribosome. *Cold Spring Harb. Perspect. Biol.* **4**, 5 (2012).
28. Nilsson, J., Sengupta, J., Frank, J. & Nissen, P. Regulation of eukaryotic translation by the RACK1 protein: A platform for signalling molecules on the ribosome. *EMBO Reports* **5**, 1137–1141 (2004).
29. Belozеров, V. E., Ratkovic, S., McNeill, H., Hilliker, A. J. & McDermott, J. C. In Vivo Interaction Proteomics Reveal a Novel p38 Mitogen-Activated Protein Kinase/Rack1 Pathway Regulating Proteostasis in Drosophila Muscle. *Mol. Cell. Biol.* **34**, 474–484 (2014).
30. Fuchs, G. *et al.* Kinetic pathway of 40S ribosomal subunit recruitment to hepatitis C virus internal ribosome entry site. *Proc. Natl. Acad. Sci.* (2015).
doi:10.1073/pnas.1421328111
31. Johnson, A. G. *et al.* Fluorescently-tagged human eIF3 for single-molecule spectroscopy. *Nucleic Acids Res.* (2018). doi:10.1063/1.102153
32. Einhauer, A. & Jungbauer, A. The FLAGTM peptide, a versatile fusion tag for the purification of recombinant proteins. *Journal of Biochemical and Biophysical Methods* (2001). doi:10.1016/S0165-022X(01)00213-5

33. Kolberg, K., Puettmann, C., Pardo, A., Fitting, J. & Barth, S. SNAP-Tag Technology: A General Introduction. *Curr. Pharm. Des.* (2013).
doi:10.2174/13816128113199990514
34. Yin, J., Lin, A. J., Golan, D. E. & Walsh, C. T. Site-specific protein labeling by Sfp phosphopantetheinyl transferase. *Nat. Protoc.* (2006). doi:10.1038/nprot.2006.43
35. Yin, J. *et al.* Genetically encoded short peptide tag for versatile protein labeling by Sfp phosphopantetheinyl transferase. *Proc. Natl. Acad. Sci.* (2005).
doi:10.1073/pnas.0507705102
36. Chiba, S., Jamal, A. & Suzuki, N. First Evidence for Internal Ribosomal Entry Sites in Diverse Fungal Virus Genomes. *Mol. Biol.* **9**, (2018).
37. Jha, S. *et al.* Trans-kingdom mimicry underlies ribosome customization by a poxvirus kinase. *Nature* (2017). doi:10.1038/nature22814

8. Appendix

Appendix 1: Viral IRES

HCV

| <i>Cell Type</i> | Haploid1 | KO #1 | KO #2 | RACK1-FLAG | RACK1-SNAP | RACK1-ybbr | ybbr-RACK1 |
|-------------------------------|---------------|-----------------|-----------------|----------------|----------------|-----------------|-----------------|
| <i>Firefly±st. dev</i> | 36863±32915 | 89779±31181 | 104581±39023 | 67959±36455 | 34756±28476 | 62089±89973 | 41163±16923 |
| <i>Renilla±st. dev</i> | 543905±547817 | 3560469±1448769 | 3219190±2854616 | 1379057±657828 | 1848698±558777 | 1811784±1437533 | 3210143±2531018 |
| <i>FF/RF±st. dev</i> | 0.0820±0.0589 | 0.0263±0.0077 | 0.0772±0.0643 | 0.0485±0.0100 | 0.0229±0.0208 | 0.0384±0.0249 | 0.0273±0.0267 |

CrPV

| <i>Cell Type</i> | Haploid1 | KO #1 | KO #2 | RACK1-FLAG | RACK1-SNAP | RACK1-ybbr | ybbr-RACK1 |
|-------------------------------|---------------|-----------------|-----------------|-----------------|-----------------|----------------|-----------------|
| <i>Firefly±st. dev</i> | 2395±2544 | 18404±19099 | 21142±37618 | 14311±8969 | 14066± | 5103±2399 | 14893±10976 |
| <i>Renilla±st. dev</i> | 315280±240727 | 2479408±3135718 | 2416706±3522303 | 1891136±1278548 | 2825086±1853942 | 1645666±572327 | 2664256±2244728 |
| <i>FF/RF±st. dev</i> | 0.0084±0.0045 | 0.0089±0.0058 | 0.0088±0.0042 | 0.0076±0.0027 | 0.0067± | 0.0032±0.0011 | 0.0080±0.0032 |

EMCV

| <i>Cell Type</i> | Haploid1 | KO #1 | KO #2 | RACK1-FLAG | RACK1-SNAP | RACK1-ybbr | ybbr-RACK1 |
|-------------------------------|---------------|-----------------|-----------------|----------------|---------------|---------------|-----------------|
| <i>Firefly±st. dev</i> | 20449±30603 | 133937±76866 | 80472±68339 | 204811±88014 | 22151±9565 | 32240±25987 | 73165±65315 |
| <i>Renilla±st. dev</i> | 166221±208897 | 2802957±1150742 | 3196043±1953769 | 2142566±834546 | 628332±74636 | 693064±382638 | 1395651±1119185 |
| <i>FF/RF±st. dev</i> | 0.1210±0.0485 | 0.04715±0.0212 | 0.0254±0.0100 | 0.0962±0.0213 | 0.0355±0.0155 | 0.0521±0.0155 | 0.0563±0.0264 |

PV

| <i>Cell Type</i> | Haploid1 | KO #1 | KO #2 | RACK1-FLAG | RACK1-SNAP | RACK1-ybbr | ybbr-RACK1 |
|------------------------------------|---------------|----------------|-----------------|----------------|----------------|---------------|-----------------|
| <i>Firefly± st. dev</i> | 26460±± | 98761±75955 | 93048±77455 | 125025±45086 | 11341±5145 | 18479±9512 | 49457±31855 |
| <i>Renilla± st. dev</i> | 252948±315912 | 1141361±733304 | 1599944±1575313 | 1412074±543885 | 1222624±426866 | 675273±467809 | 1451289±1011237 |
| <i>FF/RF± st. dev</i> | 0.1630±0.0693 | 0.0806±0.0357 | 0.0872±0.0476 | 0.0955±0.0362 | 0.0088±0.0015 | 0.0500±0.0431 | 0.0627±0.0457 |

Appendix 2: Cellular IRES

myb

| <i>Cell Type</i> | Haploid1 | KO #1 | KO #2 | RACK1-FLAG | RACK1-SNAP | RACK1-ybbr | ybbr-RACK1 |
|-------------------------------|----------------|---------------|---------------|---------------|----------------|---------------|---------------|
| <i>Firefly±st. dev</i> | 7005±4502 | 6447±2091 | 5303±5374 | 7684±2290 | 10867±10762 | 14634±9754 | 10761±9701 |
| <i>Renilla±st. dev</i> | 44251±26695 | 55129±24627 | 87864±89622 | 40651±16585 | 120594±122667 | 175176±163756 | 91934±101479 |
| <i>FF/RF±st. dev</i> | 0.1635±0.03857 | 0.1229±0.0138 | 0.0694±0.0240 | 0.2085±0.0506 | 0.0982±0.02300 | 0.1016±0.0210 | 0.1518±0.0460 |

Bag-1

| <i>Cell Type</i> | Haploid1 | KO #1 | KO #2 | RACK1-FLAG | RACK1-SNAP | RACK1-ybbr | ybbr-RACK1 |
|-------------------------------|----------------|----------------|----------------|---------------|---------------|---------------|----------------|
| <i>Firefly±st. dev</i> | 7873±1721 | 6799±1452 | 9264±6070 | 9970±4464 | 13639±3352 | 19651±16580 | 9954±2707 |
| <i>Renilla±st. dev</i> | 26721±6291 | 47631±17266 | 117595±53876 | 26557±11403 | 42117±9269 | 133060±12407 | 29890±10416 |
| <i>FF/RF±st. dev</i> | 0.2963±0.00750 | 0.1535±0.03075 | 0.0713±0.02104 | 0.3857±0.0595 | 0.3239±0.0269 | 0.1626±0.0184 | 0.3409±0.02286 |

c-myc

| <i>Cell Type</i> | Haploid1 | KO #1 | KO #2 | RACK1-FLAG | RACK1-SNAP | RACK1-ybbr | ybbr-RACK1 |
|-------------------------------|---------------|---------------|---------------|---------------|---------------|---------------|---------------|
| <i>Firefly±st. dev</i> | 16800±14231 | 8241±1786 | 6891±5146 | 11721±6409 | 17025±6693 | 18062±10162 | 14549±8554 |
| <i>Renilla±st. dev</i> | 95287±98461 | 50943±10533 | 62625±46117 | 36071±20120 | 41613±18252 | 106049±81440 | 57982±41000 |
| <i>FF/RF±st. dev</i> | 0.2423±0.0810 | 0.1626±0.0206 | 0.1138±0.0226 | 0.3374±0.0454 | 0.4163±0.0201 | 0.1901±0.0417 | 0.2692±0.0503 |

L-myc

| Cell Type | Haploid1 | KO #1 | KO #2 | RACK1-FLAG | RACK1-SNAP | RACK1-ybbr | ybbr-RACK1 |
|-------------------------------|---------------|---------------|---------------|---------------|---------------|---------------|---------------|
| <i>Firefly</i>±st. dev | 35239±18170 | 10403±9126 | 7824±4838 | 18693±7254 | 46860±16169 | 48967±20427 | 25822±7457 |
| <i>Renilla</i>±st. dev | 18296±11285 | 8660±4767 | 15887±11185 | 10480±5152 | 15618±2598 | 16587±6735 | 10031±3784 |
| <i>FF/RF</i>±st. dev | 2.5142±1.4211 | 1.0084±0.4054 | 0.5363±0.1004 | 2.6504±1.9861 | 2.9295±0.6387 | 2.9398±0.0389 | 2.9783±1.1866 |

cyclin-D

| Cell Type | Haploid1 | KO #1 | KO #2 | RACK1-FLAG | RACK1-SNAP | RACK1-ybbr | ybbr-RACK1 |
|-------------------------------|---------------|-------------|---------------|---------------|----------------|---------------|---------------|
| <i>Firefly</i>±st. dev | 10900±6565 | 4198±4308 | 3230±1884 | 5392±1610 | 13176±6617 | 14993±13153 | 10361±4209 |
| <i>Renilla</i>±st. dev | 58484±45791 | 24605±22504 | 27800±16208 | 22405±9243 | 80149.75±68599 | 96978.5±81582 | 30779±10849 |
| <i>FF/RF</i>±st. dev | 0.2274±0.0796 | 0.0491 | 0.1176±0.0086 | 0.2858±0.1223 | 0.2073±0.0543 | 0.1532±0.0169 | 0.3293±0.0266 |

Set7

| Cell Type | Haploid1 | KO #1 | KO #2 | RACK1-FLAG | RACK1-SNAP | RACK1-ybbr | ybbr-RACK1 |
|-------------------------------|----------------|----------------|----------------|----------------|----------------|----------------|----------------|
| <i>Firefly</i>±st. dev | 105631±73295 | 43948±26698 | 47298±50814 | 50100±14374 | 84713±50190 | 205186±199769 | 222568±224210 |
| <i>Renilla</i>±st. dev | 45064±22910 | 34222±16936 | 47580±33110 | 23200±9686 | 26794±18104 | 92531±98024 | 74778±80126 |
| <i>FF/RF</i>±st. dev | 2.2979±0.59619 | 1.2036±0.18548 | 0.8584±0.29910 | 2.4826±1.13101 | 3.7005±0.80241 | 2.4358±0.41979 | 3.1167±0.41623 |